AIAA AVIATION Forum
June 25-29, 2018, Atlanta, Georgia
2018 AIAA/CEAS Aeroacoustics Conference

10.2514/6.2018-2978

Amplitude scaling of turbulent-jet wavepackets

Luigi A. Antonialli* and André V. G. Cavalieri†
Instituto Tecnológico de Aeronáutica, São José dos Campos, SP, 12228-900, Brazil
Oliver T. Schmidt and Tim Colonius
California Institute of Technology, Pasadena, California, USA
Peter Jordan
Institut Pprime, France
Aaron Towne
Stanford University, California, USA
Guillaume A. Brès
Cascade Technologies, San Francisco, California, USA

Wavepackets modelling large-scale coherent structures are related to the peak noise radiation by subsonic jets. Such wavepacket models are well developed in the literature, and are often based on a linearization of the Navier-Stokes system; solutions of the resulting linear problem have a free amplitude, which can be obtained by comparison with experiments or simulations. In this work we determine amplitudes of turbulent-jet wavepackets by comparing large-eddy simulation (LES) data from Brès *et al.*[2,4] of a Mach 0.9 jet and fluctuation fields using the parabolized stability equations (PSE) model (Sasaki *et al.*[18]). Projection of the leading mode from spectral proper orthogonal decomposition (SPOD), applied to the LES data, onto the PSE model solutions is a way to determine the free amplitude, and by analyzing such amplitudes for different Strouhal numbers and azimuthal modes of the turbulent jet, it is possible to notice a clear pattern of the scaling factor with varying St. Azimuthal wavenumbers $m = 0$, 1 and 2 show an exponential dependence of wavepacket amplitude with Strouhal number. This sheds light on how wavepackets amplitudes behave and how they are excited upstream.

Nomenclature

D	Jet diameter	Re	Reynolds number
f	Frequency, Hz	γ	Heat capacity ratio
m	Azimuthal wavenumber	T	Temperature
M	Mach number	ρ	Density
U	Jet time-average streamwise velocity	c	Sound speed
θ	Azimuthal coordinates	u_θ	Azimuthal velocity component
r	Radial coordinates	u_x	Axial velocity component
x	Axial coordinates	u_r	Radial velocity component
ϕ	Polar coordinates	α	Hydrodynamic wavenumber
St	Strouhal number	ω	Frequency, rad/s
$\mathbf{q}$	Flow variables vector	$\hat{\mathbf{q}}$	Shape function of fluctuations
$\bar{\mathbf{q}}$	Mean flow variables vector	x	Axial coordinates
$\mathbf{q}'$	Flow fluctuations vector	x_o	Axial position of a cross-section

*M.Sc. Student, Divisão de Engenharia Aeronáutica, Instituto Tecnológico de Aeronáutica, AIAA Member.
†Assistant Professor, Divisão de Engenharia Aeronáutica, Instituto Tecnológico de Aeronáutica, AIAA Member.

A	Scaling factor
$\vec{\mathbf{q}}_{les}^{x_o}$	Vector of LES variables at x_o
$\vec{\mathbf{q}}_{les}^{x_o}$	Vector of PSE variables at x_o
W	Quadrature weights
$W*$	Balanced weights
N	PSE Normalization term
λ	LSE Normalization term

I. Introduction

Jet noise is a recurring theme in the aerospace community, due to the high sound pressure levels of the exhaust of jet engines, which are high enough to break windows and permanently damage human hearing. Previously it was thought that the main source of sound in jet flows was related to small eddies from the turbulent jet flow, but more recently, large-scale structures were found to be a important sound generator. These structures initially grow exponentially throught the Kelvin-Helmholtz mechanism, reach a peak, and then decay downstream, forming what is called a wavepacket. Wavepackets have been found and studied extensively in various works; further information can be found in Jordan *et al.*[11] and Cavalieri *et al.*[6]

Wavepacket models have been developed in order to predict the behaviour of jet large-scale turbulent structures, and their associated, jet noise. The parabolized stability equations (PSE), well described by Herbert[10] and Malik,[13] were initially used to describe laminar-turbulent transition in slowly-diverging flows. But as shown in Gudmunsson & Colonius[9] and Sasaki *et al.*,[18] PSE has good agreement for modeling coherent structures in turbulent jets. Key to such comparisons is the use of spectral proper orthogonal decomposition (SPOD) of flow fluctuations, as in Picard & Delville.[14] As recently shown by Towne et al.,[24] the leading SPOD mode is expected to match the optimal flow response when white-noise forcing is considered, and such optimal response can be obtained using PSE for flows with strong convective amplifications. PSE results thus compare favorably with the leading SPOD mode of the jet.

Linear PSE has solutions with a free amplitude, which must be scaled with results from experiments or numerical simulations. This can be done in an *ad hoc* way using a limited number of available measurements, or in a more theoretically-consistent manner by obtaining the amplitude of the Kelvin-Helmholtz mode near the nozzle exit by a projection using the adjoint mode.[16] Each combination of Strouhal number St and azimuthal mode m leads a separate free amplitude. How such amplitudes scale with St and m remains an open question. In the present study, we wish to explore how these wavepacket amplitudes change as a function of the said parameters. Once empirical scaling laws of wavepacket amplitude are extracted, we may infer further information on how they are excited in the flow; possible candidates involve disturbances within the nozzle boundary layer[12] and non-linear interactions with other turbulent structures.[24] It is hoped that the present analysis may help clarifying the mechanisms underpinning the excitation of Kelvin-Helmholtz wavepackets.

For that matter we will use data from the large eddy simulations (LES) of Brès et al.[2,4] Because the LES has the flexibility of providing full flow information, it is suitable for detailed comparisons with PSE results. Here, the main idea to determine the free amplitude in PSE results is to project the leading SPOD mode from LES data onto the PSE solutions to find relations and amplitudes of the model wavepacket. With this we can explore how the free amplitude of the PSE wavepackets change with St, showing indications of the mechanisms by which wavepackets are excited.

This paper is organized as follows. In section II we present the LES results and the PSE model, and also describe how the free amplitude of PSE solutions can be found using the leading SPOD mode from LES data. In section III we show some validation results for PSE, and then proceed with the determination of the wave-packet amplitudes as a function of St and m. The paper is completed with conclusions in section IV.

II. Mathematical model and numerical approach

A. Large Eddy Simulations

The simulation data is explained in Brès *et al.*[2,4] It consists of a large eddy simulation of an isothermal subsonic jet with $Re = 10^6$, coming from a converging round nozzle. The boundary layers inside the nozzle are turbulent; this is accomplished by synthetic turbulence injected at the position where a boundary layer trip is used in accompanying experiments. For the boundary layer a wall model[3] was used.

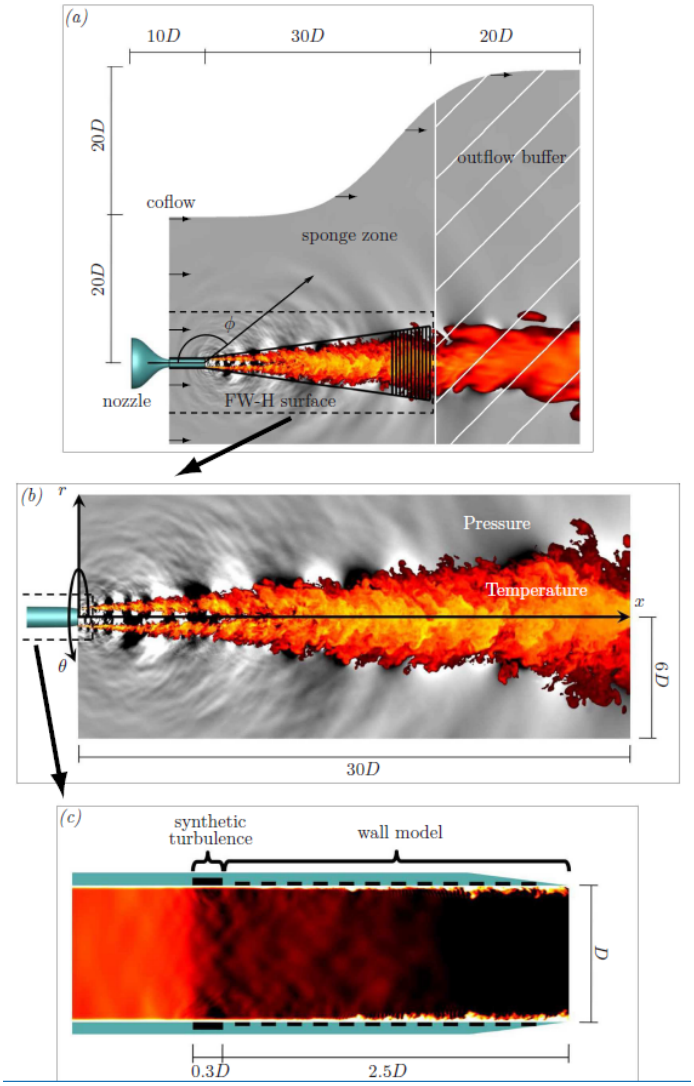

Figure 1: Jet configuration schematics, coordinates and simulation setup: (a)overview of the computational domain, (b) spatial extent of the LES database, and (c) modeling inside nozzle.

The Mach number for the simulated jet is $M = \frac{U}{c} = 0.9$ where U is the jet exit velocity and c the ambient sound speed. The azimuthal direction is labeled by θ, radial by r, x is the axial direction, and ϕ the polar direction, with center on the nozzle exit. The LES results were in close agreement with accompanying experiments, done at PPRIME Institute, Poitiers, France.[2,5]

Turbulent flow fluctuations are broadbanded. LES results are in close agreement with experimental spectral up to Strouhal number equal to 4, where Strouhal number is given by $St = \frac{fD}{U}$. For a better analysis of the flow, some post-processing was necessary. In this case a spectral proper orthogonal decomposition (SPOD) was applied to the LES data, separating it in spatial modes for each azimuthal wavenumber m and Strouhal number St. The procedure is explained in detail by Towne *et al.*[24] In what follows we will use the

leading SPOD mode from the LES data in the comparisons with PSE results.

B. Parabolized Stability Equations

The theoretical analysis of the jet is made using a wavepacket model, based on linear stability. The parabolized stability equations (PSE) are used to predict the fluctuation fields of the jet flow, using the mean field as a base flow. PSE was first developed by Bertolotti *et al.*[1] and it is used for non-parallel flows, with slow divergence in the streamwise direction, which includes jets.

Assuming a flow with properties $\mathbf{q}(x, r, \theta, t)$, it is possible to define a decomposition into an axisymmetric time-averaged component $\bar{\mathbf{q}}(x, r)$, which will be used as the base flow, and a temporal fluctuation component $\mathbf{q}'(x, r, \theta, t)$:

$$\mathbf{q}(x, r, \theta, t) = \bar{\mathbf{q}}(x, r) + \mathbf{q}'(x, r, \theta, t). \tag{1}$$

The vector $\mathbf{q}$ refers to the flow variables, $\mathbf{q} = (u_x, u_r, u_\theta, T, \rho)^T$, where u_x is the axial velocity, u_r radial velocity, u_θ azimuthal velocity, T the temperature, and ρ the density, all in cylindrical coordinates. The jet is considered non-swirling, therefore there is no mean azimuthal velocity component u_θ.

In Gaster[8] and Crighton & Gaster[7] an appropriate *Ansatz* for the fluctuations is derived, and given by:

$$\mathbf{q}'(x, r, \theta, t) = \hat{\mathbf{q}} e^{i \int_{x_0}^{x} \alpha(\xi) d\xi} e^{im\theta} e^{-i\omega t}. \tag{2}$$

In equation (2) the term $\alpha(\xi)$ is the complex-valued hydrodynamic wavenumber that varies with axial direction; its imaginary part is related to exponential growth or decay of fluctuations. m is the azimuthal wavenumber, and ω is the frequency of the fluctuations. This *Ansatz* has a slowly-changing part for the fluctuations $\hat{\mathbf{q}}(x, r)$ and a fast part, $e^{i \int_{x_0}^{x} \alpha(\xi) d\xi}$. $\hat{\mathbf{q}}(x, r)$ is the shape function of the fluctuation amplitude, which varies slowly in the streamwise direction. The fast part is the oscillatory characteristic of the large scale turbulent structures. The combination of these two parts generates fluctuations in the shape of a wavepacket.

To obtain the values of $\alpha(\xi)$ and $\hat{\mathbf{q}}(x, r)$, the *Ansatz* from equation (2) is substituted in a matrix system with the linearised, compressible, continuity, Euler, and energy equations, resulting in a system that can be cast in matrix form as:

$$\left[A(\bar{\mathbf{q}}, \alpha, \omega) + B(\bar{\mathbf{q}})\right] \hat{\mathbf{q}} + C(\bar{\mathbf{q}}) \frac{\partial \hat{\mathbf{q}}}{\partial x} + D(\bar{\mathbf{q}}) \frac{\partial \hat{\mathbf{q}}}{\partial r} = 0. \tag{3}$$

The complete procedure and description of every term is in Gudmundsson & Colonius.[9] The PSE code used to generate the present results is fully described in Sasaki *et al.*[18] The initial fluctuation profile, in the nozzle exit plane, is given by linear stability theory and then marched downstream by the PSE. For this case the base flow used is a time-averaged mean flow taken from the large eddy simulation, described in the previous section.

In the present study, we are interested in determining the behavior of wave-packet amplitudes as a function of St and m. For that matter, the linear PSE solutions should be normalized in a definite way. We have adopted as a normalization condition that flow fluctuations at the nozzle exit have unit norm. This is ensured by calculating

$$\hat{\mathbf{q}}_0^H \, diag\left(W\bar{\rho}_0, W\bar{\rho}_0, W\bar{\rho}_0, W\frac{\bar{T}_0}{\gamma\bar{\rho}_0 M^2}, \frac{\bar{\rho}_0}{\gamma(\gamma-1)\bar{T}_0 M^2}\right) \hat{\mathbf{q}}_0 = \hat{\mathbf{q}}_0^H W^* \hat{\mathbf{q}}_0 = N^2, \tag{4}$$

where the subscript $_0$ are the properties of the flow near the nozzle or $x = 0$, W are quadrature weights, W^* the balanced weights, and N the normalization term. Therefore the normalized PSE solutions are given as:

$$\hat{\mathbf{q}}_{norm} = \frac{\hat{\mathbf{q}}}{N}. \tag{5}$$

After the normalization, the pressure can be calculated by:

$$\hat{\mathbf{P}} = \frac{(\gamma - 1)}{\gamma} \left(\bar{\rho}\hat{T}_{norm} + \bar{T}\hat{\rho}_{norm}\right). \tag{6}$$

C. Projection of LES onto PSE Results

The numerical solutions of linear PSE are normalized as described in the previous section. But this leads to an arbitrary amplitude, and comparison with LES results requires rescaling this amplitude with simulation data. We have taken the values along a cross-section of the jet to calculate a scaling factor between the first SPOD mode from the LES and PSE results. This scaling factor A will be multiplied to the whole PSE solution to adjust the free amplitude of linear PSE solutions.

The term $\vec{\mathbf{q}}_{pse}^{x_o}(r)$ is a vector of any fluctuation calculated by the PSE model (for instance, velocity or pressure, and already normalized) along the r direction for a given position x_o, and $\vec{\mathbf{q}}_{les}^{x_o}(r)$ the vector of the same quantity, taken from the first SPOD mode of the LES, for the same position x_o. We assume that the LES data can be written as:

$$\vec{\mathbf{q}}_{les}^{x_o}(r)\sqrt{\lambda} = A\vec{\mathbf{q}}_{pse}^{x_o}(r). \tag{7}$$

where λ is the LES amplitude that was used for normalization during the SPOD calculation, and it needs to be multiplied for a physical realistic value, better shown in Sinha *et al.*[22] Applying an inner product in equation (7), it is possible to find a scalar value for A:

$$\langle \vec{\mathbf{q}}_{les}^{x_o}(r), \vec{\mathbf{q}}_{pse}^{x_o}(r)\rangle = A\langle \vec{\mathbf{q}}_{pse}^{x_o}(r), \vec{\mathbf{q}}_{pse}^{x_o}(r)\rangle,$$

$$A = \frac{\langle \vec{\mathbf{q}}_{les}^{x_o}(r), \vec{\mathbf{q}}_{pse}^{x_o}(r)\rangle}{\langle \vec{\mathbf{q}}_{pse}^{x_o}(r), \vec{\mathbf{q}}_{pse}^{x_o}(r)\rangle}, \tag{8}$$

where the inner product is defined by:

$$\langle f(r), g(r)\rangle = \int_0^\infty (f(r)\cdot g^*(r))r dr. \tag{9}$$

The trapezoid rule is used to calculate the integral. PSE uses a different grid from the LES results, and therefore an interpolation was required to obtain values for the same x_o.

This factor A was then calculated for a range of St varying from near 0 to 3, then plotted to visualize $A(St)$. The x_o positions to be analyzed were based on the results of Sasaki *et al.*,[17] and were chosen for positions of close agreement between PSE and LES. The resulting values of $A(St)$ can be used to infer the frequency dependence of wave-packet amplitudes.

Unlike global stability modes, linear PSE does not provide a basis for flow fluctuations; PSE results are the solution of a boundary-value problem, with non-zero boundary conditions at the nozzle exit, and not eigenfunctions of a linear operator. Hence, strictly speaking, one cannot think of the procedure above as a projection as often done for stability eigenfunctions.[15,16] However, we are here interested in the determination of the amplitude of a single spatial function, and thus the approach can be used as method to estimate wave-packet amplitudes considering a jet slice at x_o. Notice that in the upstream region both the SPOD mode and the PSE solution have similar growth rates, and because of this the amplitude parameter A is expected to depend only weakly on the choice of x_o.

III. Results

A. PSE validation

The first step was to obtain PSE wavepackets and validate them by comparison with the first POD mode from the LES data. The code was setup to run for Mach number 0.9, for St varying from 0.0868 to 2.778. The Strouhal numbers used are the same as the ones in the LES results to facilitate comparison. For initial analysis, the first 3 azimuthal modes where calculated ($m = 0, 1, 2$). A comparison of pressure fluctuations is done for 3 different St, 0.5, 1.0 and 2.4, and results are shown in figures 2–4.

We notice that there is a close agreement between the PSE and the first SPOD modes for a good range of frequencies. The same code presented by Sasaki *et al.*[18] showed great agreement for Strouhal number as high as 4, shown in Sasaki *et al.*[19] This validates the PSE results for modeling turbulent-jet wavepackets for the present flow.

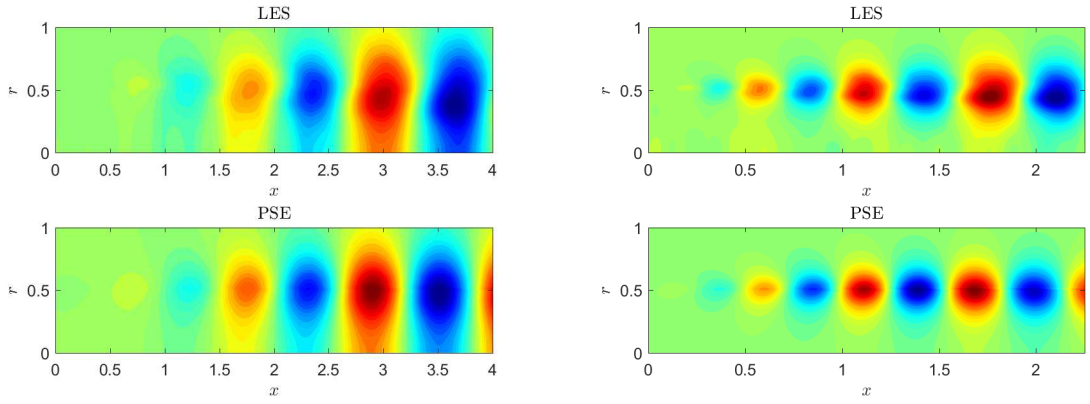

(a) $St = 0.5$ (b) $St = 1$

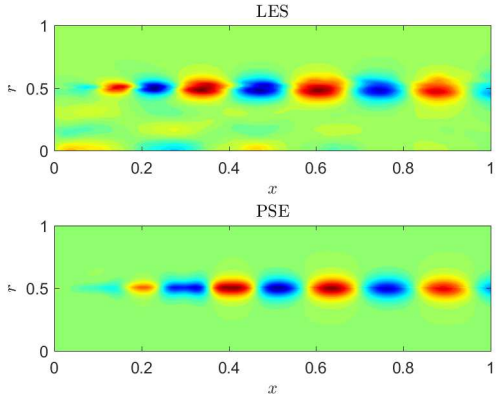

(c) $St = 2.4$

Figure 2: Pressure fluctuation contour for axyssimetric mode ($m = 0$) for Strouhal number (a) $St = 0.5$, (b) $St = 1$, (c) $St = 2.4$.

B. Scaling of wavepacket amplitude

A range of cross-section was selected based on the observed agreement between PSE and LES, varying from $x/D = x_o = 0.5$ to $x_o = 1.5$. The scalar factor A was calculated for pressure fluctuations, for the first 3 azimuthal modes ($m = 0, 1, 2$). Amplitude values for St in $[0.086806, 2.4306]$, and plotted in figure 5. For low Strouhal numbers (such as St=0.1 and 0.2) the PSE does not have good agreement with the leading SPOD mode, as observed in prior works.[6,21] This leads to an almost random behavior for A, as seen in the figure 5 (Only shown for $m = 0$, since for $m = 1, 2$ teh behavior is similar). Therefore a shorter Strouhal number range $[0.43403, 2.4306]$ was used to show the amplitude behavior with St. The results, plotted in semilog scale, show an exponential decay of amplitudes with increasing St. The amplitudes present some oscillatory behavior with St. At least part of this behavior can be attributed to trapped acoustic modes present in the M = 0.9 flow, as explained in Towne et al.[23] and Schmidt et al.[20] There are amplitude peaks in figure 6, which coincide with the St for trapped waves, highlighted in the figure by the blue arrows.

A exponential fit was then chosen to represent the $A(St)$ behavior. To use characteristics of all the cross-sections calculated for the fitting, all the values for each cross-section x_o and each St were shown in a scatter plot (represented in figure 7 by the red crosses), and then an exponential fit was made. Resulting fits are given as:

$$A(St) = 5.15 \cdot 10^{-4} \mathrm{e}^{-2.75St}, \quad m = 0 \tag{10}$$

$$A(St) = 3.72 \cdot 10^{-4} \mathrm{e}^{-2.64St}, \quad m = 1 \tag{11}$$

$$A(St) = 1.81 \cdot 10^{-3} \mathrm{e}^{-2.27St}, \quad m = 2 \tag{12}$$

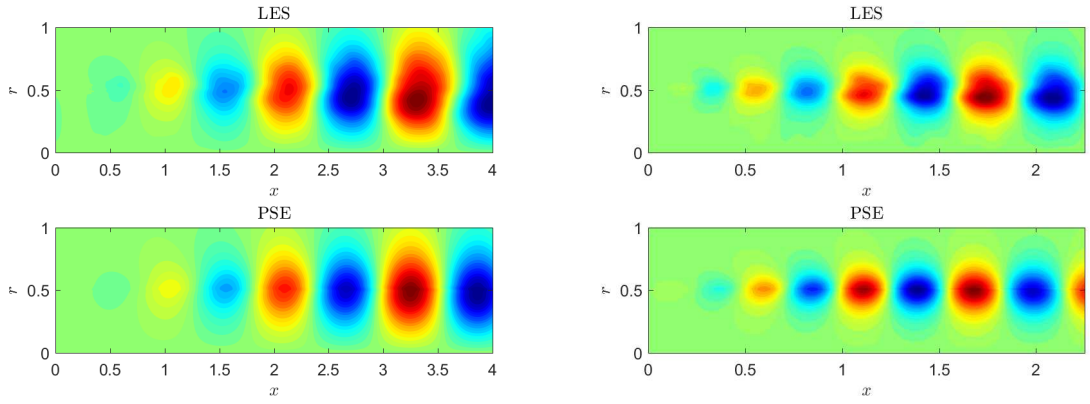

(a) $St = 0.5$ (b) $St = 1$

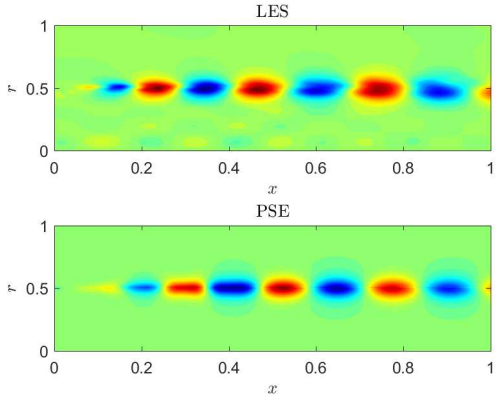

(c) $St = 2.4$

Figure 3: Pressure fluctuation contour for azimuthal mode $m = 1$ for Strouhal number (a) $St = 0.5$, (b) $St = 1$, (c) $St = 2.4$.

The obtained Strouhal-number dependence can be used to estimate power spectra at given positions of the flow. An example is shown in figure 8, where pressure spectra on the jet centerline are calculated using linear PSE results scaled with the expression in eqs. (10)—(12). Results show the expected qualitative trends, albeit with a sharp decay for high St, probably due to the dominance of other flow structures for those high frequencies at a given location.

The present results were obtained by considering solely pressure fluctuations in the determination of the amplitude described in section IIc. The same approach was also applied considering the streamwise velocity, and nearly identical results were obtained; these are not shown here for brevity.

IV. Conclusion

The frequency dependence of turbulent jet wave-packet amplitudes is studied by an approach consisting of the projection of the leading SPOD mode from a well validated large-eddy simulation onto linear PSE results. This procedure, which is applied for jet cross-sections where linear PSE has been shown to agree with numerical and experimental data, leads to wave-packet amplitudes with an exponential dependence with Strouhal number. Exponential fits are obtained for azimuthal wavenumbers $m = 0$, 1 and 2, and may be useful in the estimation of power spectra of flow fluctuations using PSE results.

The present results may serve as a basis to study the receptivity mechanisms of Kelvin-Helmholtz wavepackets in turbulent jets. An open question regarding such wavepackets is related to their excitation; this has been explored by Kaplan et al.[12] but requires further study. The exponential dependence

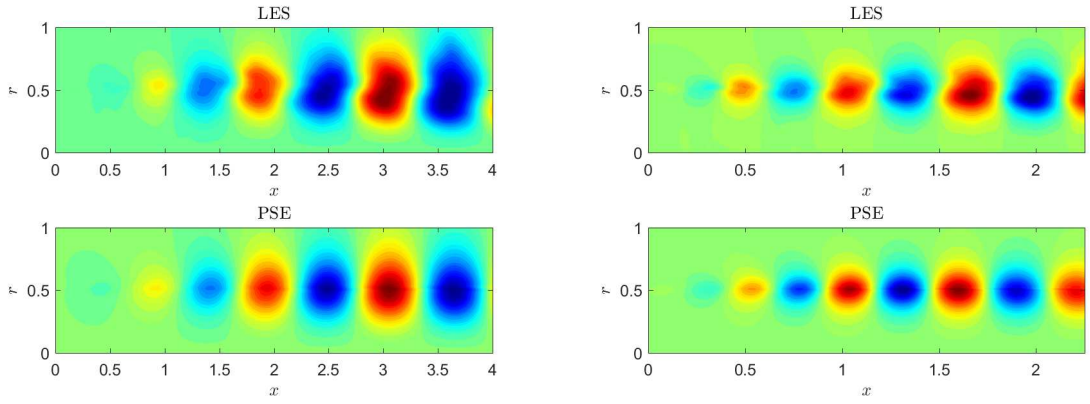

(a) $St = 0.5$ (b) $St = 1$

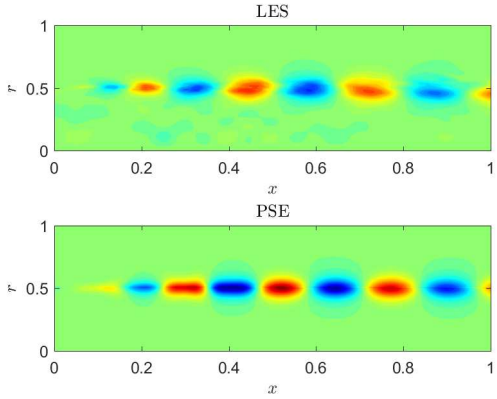

(c) $St = 2.4$

Figure 4: Pressure fluctuation contour for azimuthal mode $m = 2$ for Strouhal number (a) $St = 0.5$, (b) $St = 1$, (c) $St = 2.4$.

seen here can serve as a test of proposed mechanisms and models, which should be able to reproduce the amplitude scaling observed in the results. Ongoing work includes the extension of this analysis to other jet Mach numbers, which will lead to a more complete characterization of the amplitudes of jet wavepackets.

References

[1]F. Bertolotti, T. Herbert, and P. Spalart. Linear and nonlinear stability of the blasius boundary layer. *Journal of Fluid Mechanics*, 242:441–474, 1992.

[2]G. Brès, P. Jordan, V. Jaunet, M. Le Rallic, A. Cavalieri, A. Towne, S. Lele, T. Colonius, and O. Schmidt. Importance of the nozzle-exit boundary-layer state in subsonic turbulent jets. *Journal of Fluid Mechanics*, 2018.

[3]G. A. Brès, F. E. Ham, J. W. Nichols, and S. K. Lele. Nozzle wall modeling in unstructured large eddy simulations for hot supersonic jet predictions. *AIAA paper*, 2142:2013, 2013.

[4]G. A. Brès, F. E. Ham, J. W. Nichols, and S. K. Lele. Unstructured large-eddy simulations of supersonic jets. *AIAA Journal*, 2017.

[5]G. A. Brès, V. Jaunet, M. Le Rallic, P. Jordan, A. Towne, O. Schmidt, T. Colonius, A. V. Cavalieri, and S. K. Lele. Large eddy simulation for jet noise: azimuthal decomposition and intermittency of the radiated sound. *AIAA Paper*, 3050:2016, 2016.

[6]A. V. Cavalieri, D. Rodríguez, P. Jordan, T. Colonius, and Y. Gervais. Wavepackets in the velocity field of turbulent jets. *Journal of Fluid Mechanics*, 730:559–592, 2013.

[7]D. Crighton and M. Gaster. Stability of slowly diverging jet flow. *Journal of Fluid Mechanics*, 77(02):397–413, 1976.

[8]M. Gaster. On the effects of boundary-layer growth on flow stability. *Journal of Fluid Mechanics*, 66(03):465–480, 1974.

[9]K. Gudmundsson and T. Colonius. Instability wave models for the near-field fluctuations of turbulent jets. *Journal of Fluid Mechanics*, 689:97–128, 2011.

[10]T. Herbert. Parabolized stability equations. *Annual Review of Fluid Mechanics*, 29(1):245–283, 1997.

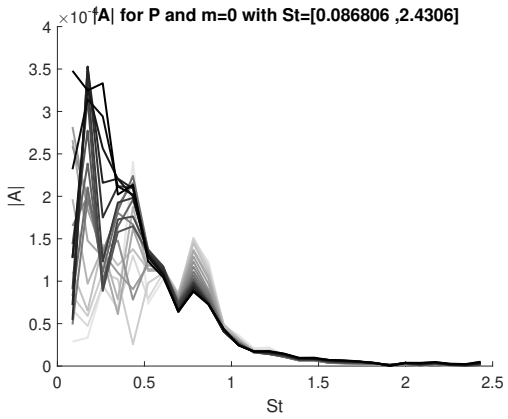

Figure 5: Scaling factor of pressure fluctuations for $St = [0.086806, 2.4306]$ for azimuthal mode $m = 0$, with x/D varying form $x/D = 0.5$ (grey) to $x/D = 1.5$ (black).

[11]P. Jordan and T. Colonius. Wave packets and turbulent jet noise. *Annual review of fluid mechanics*, 45:173–195, 2013.

[12]O. Kaplan, P. Jordan, and A. V. Cavalieri. Exploring the link between nozzle dynamics and wavepackets in a mach 0.9 turbulent jet. In *23rd AIAA/CEAS Aeroacoustics Conference*, page 3708, 2017.

[13]M. Malik, S. Chuang, and M. Hussaini. Accurate numerical solution of compressible, linear stability equations. *Zeitschrift für angewandte Mathematik und Physik ZAMP*, 33(2):189–201, 1982.

[14]C. Picard and J. Delville. Pressure velocity coupling in a subsonic round jet. *International Journal of Heat and Fluid Flow*, 21(3):359–364, 2000.

[15]D. Rodríguez, A. V. Cavalieri, T. Colonius, and P. Jordan. A study of linear wavepacket models for subsonic turbulent jets using local eigenmode decomposition of piv data. *European Journal of Mechanics-B/Fluids*, 49:308–321, 2015.

[16]D. Rodríguez, A. Sinha, G. A. Brès, and T. Colonius. Inlet conditions for wave packet models in turbulent jets based on eigenmode decomposition of large eddy simulation data. *Physics of Fluids*, 25(10):105107, 2013.

[17]K. Sasaki, A. V. Cavalieri, P. Jordan, O. T. Schmidt, T. Colonius, and G. A. Brès. High-frequency wavepackets in turbulent jets. *Journal of Fluid Mechanics*, 830, 2017b.

[18]K. Sasaki, S. Piantanida, A. V. Cavalieri, and P. Jordan. Real-time modelling of wavepackets in turbulent jets. In *21th AIAA/CEAS Aeroacoustic Conference and Exhibit*, 2015.

[19]K. Sasaki, S. Piantanida, A. V. Cavalieri, and P. Jordan. Real-time modelling of wavepackets in turbulent jets. *Journal of Fluid Mechanics*, 821:458–481, 2017.

[20]O. Schmidt, A. Towne, T. Colonius, A. Cavalieri, P. Jordan, and G. Brès. Wavepackets and trapped acoustic modes in a turbulent jet: coherent structure eduction and global stability. *Journal of Fluid Mechanics*, 825(1):1153–1181, 2017.

[21]O. T. Schmidt, A. Towne, G. Rigas, T. Colonius, and G. A. Brès. Spectral analysis of jet turbulence. *arXiv preprint arXiv:1711.06296*, 2017.

[22]A. Sinha, D. Rodríguez, G. A. Brès, and T. Colonius. Wavepacket models for supersonic jet noise. *Journal of Fluid Mechanics*, 742:71–95, 2014.

[23]A. Towne, A. V. Cavalieri, P. Jordan, T. Colonius, O. Schmidt, V. Jaunet, and G. A. Brès. Acoustic resonance in the potential core of subsonic jets. *Journal of Fluid Mechanics*, 825:1113–1152, 2017.

[24]A. Towne, O. T. Schmidt, and T. Colonius. Spectral proper orthogonal decomposition and its relationship to dynamic mode decomposition and resolvent analysis. *arXiv preprint arXiv:1708.04393*, 2017.

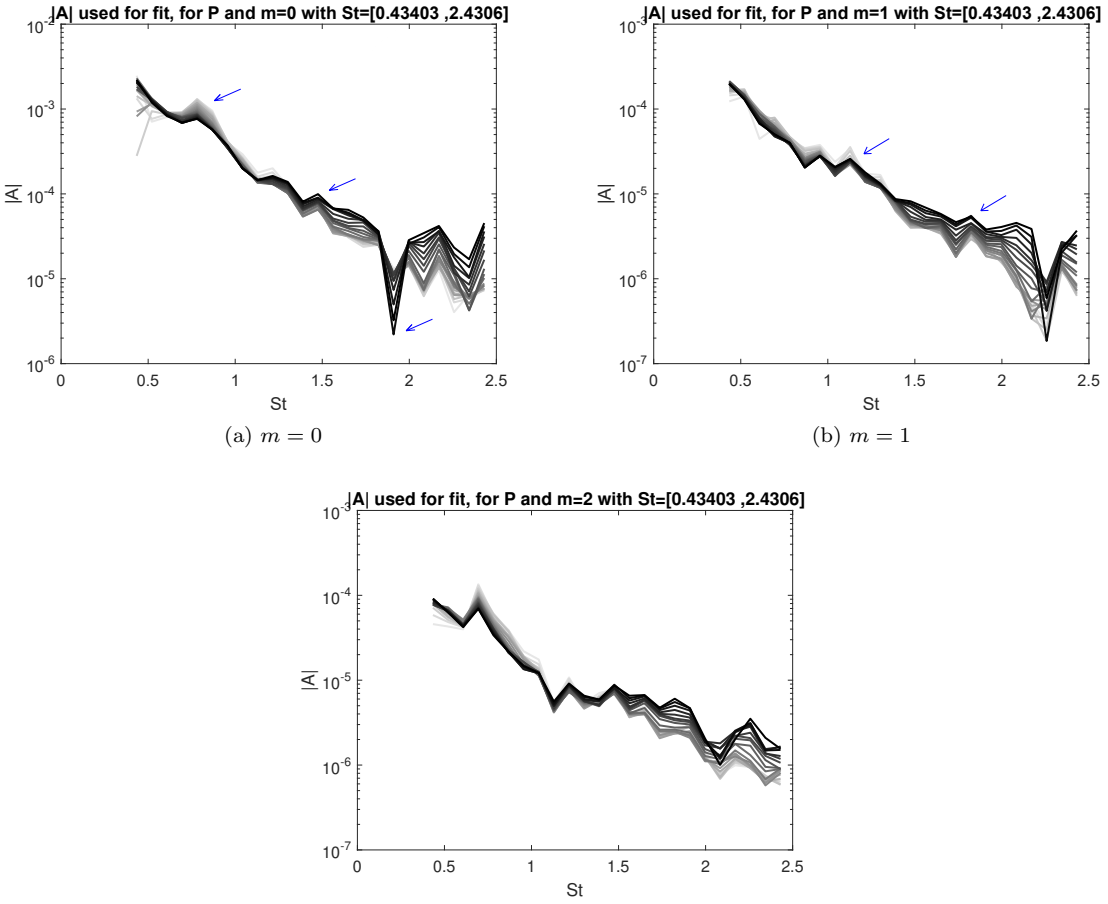

(a) $m = 0$

(b) $m = 1$

(c) $m = 2$

Figure 6: Scaling factor of pressure fluctuations for $St = [0.43403, 2.4306]$ for azimuthal mode $m = 0, 1, 2$ in semilog scale, with x/D varying form $x/D = 0.5$ (grey) to $x/D = 1.5$ (black). Strouhal numbers of resonant trapped acoustic waves[23] are shown with blue arrows.

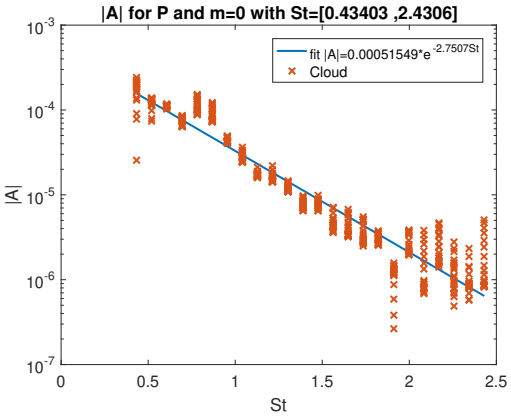

(a) $m = 0$

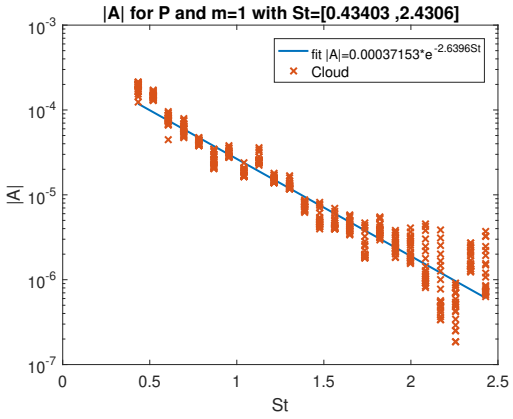

(b) $m = 1$

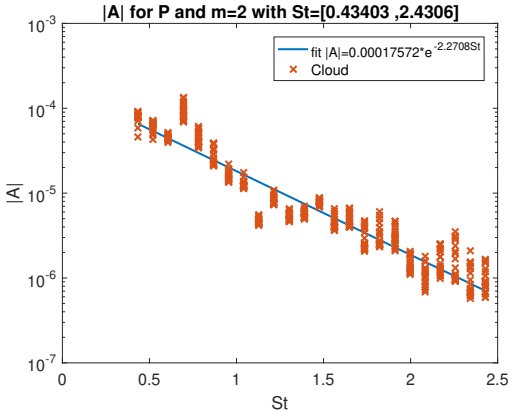

(c) $m = 2$

Figure 7: Point cloud and fit of scaling factor of pressure fluctuations for $St = [0.43403, 2.4306]$ for azimuthal mode $m = 0, 1, 2$ in semilog scale.

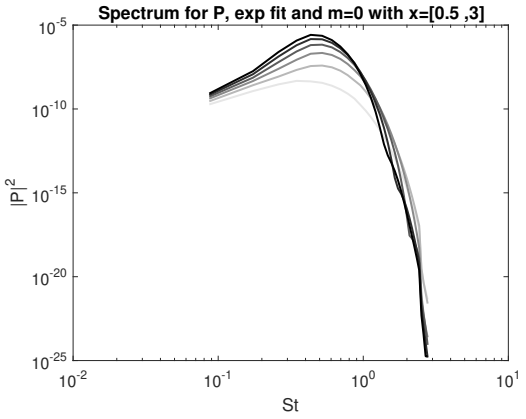

(a) $m = 0$

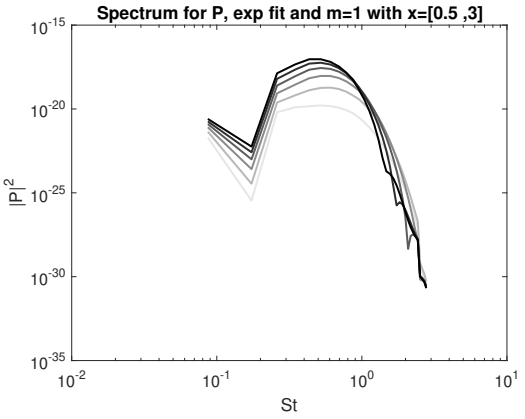

(b) $m = 1$

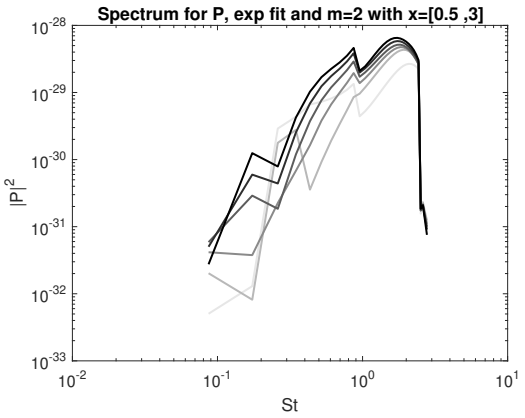

(c) $m = 2$

Figure 8: Centerline spectrum using the scaling factor of pressure fluctuations for $St = [0.086806, 2.778]$ for azimuthal mode $m = 0, 1, 2$ in semilog scale, with x/D varying form $x/D = 0.5$ (grey) to $x/D = 3$ (black).